

**DEVELOPMENT OF A VARIABLE DIAMETER WHEEL FOR  
MOTION TRANSMISSION**

By

José Emilio Lugo Ortiz

A thesis submitted in partial fulfillment of the requirements for the degree of

MASTER OF SCIENCE

in

MECHANICAL ENGINEERING

UNIVERSITY OF PUERTO RICO  
MAYAGÜEZ CAMPUS

May, 2009

Approved by:

---

David Serrano, Sc.D  
Member, Graduate Committee

---

Date

---

Frederick Just, Ph.D  
Member, Graduate Committee

---

Date

---

David Dooner, Ph.D  
President, Graduate Committee

---

Date

---

Pedro Vásquez, Ph.D  
Representative of Graduate Studies

---

Date

---

Pablo Cáceres, Ph.D  
Chairperson of the Department

---

Date

Abstract of Dissertation Presented to the Graduate School  
of the University of Puerto Rico in Partial Fulfillment of the  
Requirements for the Degree of Master of Science

**DEVELOPMENT OF A VARIABLE DIAMETER WHEEL FOR  
MOTION TRANSMISSION**

By

José Emilio Lugo Ortiz

May 2009

Chair: David Dooner  
Major Department: Mechanical Engineering

In this work a variable diameter wheel (VDW) is presented. Two VDWs are combined in a manner where motion can be transmitted between these VDWs. The scope is limited to a kinematics analysis of a mechanism consisting of two VDWs. First the VDW is explained using a patent submitted by Charles Hoberman. Then a mechanism couples each wheel to a shaft. This mechanism controls the diameter of the wheels. Further, a sub-mechanism is designed to synchronize the change in wheel diameters in order for them to remain in contact.

The sub-mechanism consists of a rotating plate with grooves. Coordinate transformations are used to obtain groove paths that synchronize each wheel diameter. The mobility of the entire mechanism is determined. Subsequently, a vector loop equation is written to obtain the VDW dimensions. After the entire mechanism is developed, certain design parameters that affect speed ratio range are explored. At the end, possible motion transmission means between wheels are suggested.

Resumen de Disertación Presentado a Escuela Graduada  
de la Universidad de Puerto Rico como requisito parcial de los  
Requerimientos para el grado de Maestría en Ciencias

## **DESARROLLO DE UNA RUEDA CON DIÁMETRO VARIABLE PARA TRANSMITIR MOVIMIENTO**

Por

José Emilio Lugo Ortiz

Mayo 2009

Consejero: David Dooner  
Departamento: Ingeniería Mecánica

En este trabajo se desarrolla una rueda con diámetro variable (RDV). Dos RDV son combinadas de tal manera que se puede transmitir movimiento entre ambas. Este trabajo en general se limita a los análisis cinemáticos de dos RDV. La primera parte se dedica a explicar la RDV usando una patente de autoría de Charles Hoberman. Luego, se diseña un mecanismo que acopla la rueda a los ejes; a la misma vez, este mecanismo controla el diámetro de la rueda. Por consiguiente, un sub-mecanismo se diseña para que sincronice ambas ruedas para que se mantengan en contacto.

Para todos los mecanismos envueltos se realizaron estudios de movilidad y bucles de vectores. El sub-mecanismo consiste en una placa con surcos que rota. Se utilizaron transformaciones de coordenadas para poder obtener el surco necesario para controlar el desplazamiento axial de los dos componentes que controlan el diámetro de cada RDV. Una vez el diseño está terminado, se explora cuáles son los parámetros de diseño que más afectan el rango de la relación de engranajes. Al final, se mencionan posibles medios entre rueda y rueda para que estas pasen el movimiento de una a la otra.

Copyright © 2009

by

José Emilio Lugo Ortiz

To God who gave me the gift of life.

To my wife and family who gave me unconditional love and support throughout  
this exceptional journey.

## ACKNOWLEDGMENTS

I would like to thank my advisor Dr. David Dooner for his honest and sincere guidance and support during my Master's thesis.

I wish to thank Dr. Frederick Just for his input as member of my committee. I would like to express my special thanks to him for being a good patient teacher to explain control problems during the time I was working as a teaching-assistant in his class. Also I wish to thank Dr. David Serrano for his input as a member of my committee and for his previous counseling as Formula SAE advisor.

Finally, I would like to thank the Department of Mechanical Engineering at the University of Puerto Rico-Mayagüez for their academic support and the GEM-GM consortium for their financial support. Also I would like to thank the Partners for the Advancement of Collaborative Engineering Education for Software and Hardware support.

## TABLE OF CONTENTS

	<u>page</u>
ABSTRACT ENGLISH . . . . .	ii
ABSTRACT SPANISH . . . . .	iii
ACKNOWLEDGMENTS . . . . .	vi
LIST OF TABLES . . . . .	ix
LIST OF FIGURES . . . . .	x
LIST OF ABBREVIATIONS . . . . .	xii
LIST OF SYMBOLS . . . . .	xiii
<b>1 INTRODUCTION . . . . .</b>	<b>1</b>
1.1 Research Motivation . . . . .	1
1.2 Objectives . . . . .	2
1.3 Procedure . . . . .	2
<b>2 LITERATURE REVIEW . . . . .</b>	<b>3</b>
2.1 Continuously Variable Transmission . . . . .	3
2.1.1 Belt CVT and Chain CVT . . . . .	3
2.1.2 Toroidal CVT . . . . .	4
2.1.3 Hydrostatic CVT . . . . .	5
2.1.4 Ratcheting CVT . . . . .	5
2.1.5 Variable Toothed Wheel Transmission . . . . .	6
2.2 Hoberman Patent . . . . .	7
<b>3 HOBERMAN WHEEL . . . . .</b>	<b>9</b>
3.1 Description . . . . .	9
3.2 Degrees of Freedom Analysis . . . . .	11
3.3 Position Vector Loop . . . . .	12
<b>4 VARIABLE DIAMETER WHEEL MECHANISM . . . . .</b>	<b>16</b>
4.1 Wheel-Shaft Mechanism . . . . .	16
4.1.1 Degrees of Freedom Analysis . . . . .	17
4.1.2 Position Vector Loop . . . . .	18
4.2 Motion Transmission Mechanism . . . . .	19

4.3	Sliders Control Mechanism . . . . .	21
4.3.1	Degrees of Freedom Analysis . . . . .	21
4.3.2	Position Vector Loop . . . . .	21
4.4	Motion Transmission . . . . .	25
4.4.1	Gear Ratio Range . . . . .	25
5	Design Methodology . . . . .	26
5.1	Wheel Ratio Range . . . . .	26
5.2	CD constrained . . . . .	28
6	CONCLUSIONS AND FUTURE WORKS . . . . .	30
6.1	Conclusions . . . . .	30
6.2	Future Work . . . . .	30
6.2.1	Motion Transmission Mediums . . . . .	30
	APPENDICES . . . . .	33
A	MatLabCodes . . . . .	34
A.1	Main Code . . . . .	34
A.2	Secant Method Function . . . . .	37
A.3	Gear ratio range . . . . .	38
A.4	Maximum and Minimum radius function . . . . .	39
A.5	Maximum and Minimum radius function . . . . .	41
B	NX 5 Models . . . . .	44
B.1	Screen shots of NX 5 Model changing ratios . . . . .	44

LIST OF TABLES

<u>Table</u>		<u>page</u>
3-1	Wheel Values Table . . . . .	14
4-1	Nomenclature Table . . . . .	20
4-2	Coordinate Transformation Values Table . . . . .	24

## LIST OF FIGURES

<u>Figure</u>	<u>page</u>
2-1 V-belt CVT [7] . . . . .	4
2-2 Toroidal CVT [8] . . . . .	5
2-3 Diagram of a Hydrostatic CVT. . . . .	5
2-4 Ratcheting CVT [9] . . . . .	6
2-5 Cross-section of iCVT variator internals [10] . . . . .	7
2-6 Succession of perspective views of a complete faceted icosahedral structure [5]. . . . .	8
3-1 Hoberman wheel . . . . .	9
3-2 Strut element . . . . .	10
3-3 Scissor pair . . . . .	10
3-4 Hoberman Wheel . . . . .	11
3-5 Kinematic scissor pair diagram . . . . .	12
3-6 Scissor pair vector loop . . . . .	13
3-7 Outer radius vs inner radius of a scissor pair . . . . .	14
3-8 Scissor angle vs inner radius . . . . .	15
4-1 Variable diameter wheel mechanism . . . . .	16
4-2 Wheel-shaft mechanism . . . . .	17
4-3 Kinematic wheel-shaft diagram . . . . .	17
4-4 Wheel-shaft vector loop . . . . .	18
4-5 Motion Transmission Mechanism . . . . .	19
4-6 Motion transmission mechanism nomenclature diagram . . . . .	20
4-7 Controller mechanism diagram . . . . .	21
4-8 Controller mechanism vector loop . . . . .	22

4-9	Coordinate systems diagram . . . . .	23
4-10	Rocker groove path. . . . .	24
4-11	Gear ratio range for the specific arrangement. . . . .	25
5-1	Gear ratio range vs $\eta$ and $l_{ab}$ . . . . .	27
5-2	Different $CD$ . . . . .	27
5-3	Minimum radius . . . . .	28
6-1	Gear ratio range for the specific arrangement. . . . .	31
6-2	Gear ratio range for the specific arrangement. . . . .	32
B-1	. . . . .	44
B-2	. . . . .	44
B-3	. . . . .	45
B-4	. . . . .	45
B-5	. . . . .	45

## LIST OF ABBREVIATIONS

CVT	Continuously Variable Transmission
VDP	Variable-Diameter Pulley
DOF	Degrees of Freedom
AWD	All Wheel Drive
CAD	Computer Aided Drawing
CD	Center Distance
iCVT	Incremental Continuously Variable Transmission
VDW	Variable Diameter Wheel
IWSI	Input Wheel Slider Input
IWSO	Input Wheel Slider Output
IWIR	Input Wheel Inner Radius
IWOR	Input Wheel Outer Radius
OWSI	Output Wheel Slider Input
OWSO	Output Wheel Slider Output
OWIR	Output Wheel Inner Radius
OWOR	Output Wheel Outer Radius

## LIST OF SYMBOLS

$\alpha$	Strut angle.
$\eta$	Number of scissor pairs.
$\beta$	Normal angle.
$\lambda$	Scissors angle.
$M$	Mobility.
$j$	Number of joints.
$l$	Number of links.
$f_i$	Joint DOF.
$R_{inner}$	Inner radius of Hoberman wheel.
$R_{outer}$	Outer radius of Hoberman wheel.
$l_{ab}$	Length of strut element.
$\gamma$	Scissors angle
$b_x$	X coordinate of point b.
$S_{output}$	Slider output.
$S_{input}$	Slider input.
$l_{ab}$	Length of link cd.
$l_{da}$	Length of wheel holder link.
$r_n$	Position vector of the new coordinate system.
$r_m$	Position vector of the old coordinate system.
$M_{nm}$	Coordinate transformation matrix.
$e_x$	X coordinate of point e.
$\theta$	Angle between old and new axis.
$\Delta x$	Length between old and new x axis.
$sr$	Speed ratio.
$srr$	Speed ratio range.
$R_{max}$	Maximum radius of wheel.
$R_{min}$	Minimum radius of wheel.

# CHAPTER 1

## INTRODUCTION

“If I can’t picture it, I can’t understand it.” -Albert Einstein

### 1.1 Research Motivation

The rising energy cost and need to conserve and optimize the use of energy justify research for more efficient machine components. Transportation equipment is composed of many machine components. If the efficiency of transportation equipment is increased the greenhouse gas emissions from transportation can have significant reductions. It has been found that from all the systems of transportation equipment the single largest contribution to improve fuel efficiency is expected to come from the drive train [1].

Most gears pairs are 98%-99% efficient themselves [2]. In vehicles the power source (eg. Internal Combustion Engines) has an optimum point or region of maximum efficiency. When the power source is coupled to the output shaft by a gear transmission, only a fixed number of gear ratios are attained and the power source cannot be operated all the time at that optimum point. In order to increase efficiency of the overall system, gear ratios have to change between the power source and the output shaft. These changes can maintain the Internal Combustion engine running at its optimum point while the vehicle runs at different speeds.

The development of a variable diameter wheel mechanism used as part of a transmission mechanism can improve the fuel efficiency of transportation equipment. A variable diameter wheel system, can maintain the power source that is coupled to

the input shaft running at the optimum point of the power source while the output shaft can have various output speeds.

## 1.2 Objectives

The goal is to design a mechanism with a pseudo circular shape that will change its diameter. This mechanism will connect to a sibling mechanism, making possible the transmission of motion. The usefulness of this mechanism will be a function of how well it can transmit torque (load) and how wide the gear ratio range can be.

The proposed work will meet the following objectives:

1. Design a mechanism with a pseudo circular shape that will change its diameter.
2. Calculate the position of every link of the mechanism.
3. Find the best center distance for a wheel arrangement
4. Find the optimum wheel arrangement for a constrained center distance

## 1.3 Procedure

The proposed research work is divided in the following stages:

1. Literature review.
  - (a) CVT literature review.
  - (b) Hoberman patent review.
2. Mobility analysis.
3. Vector loop.
4. Mathematical model of both wheels moving.
5. Mathematical model for the valid ranges of the links for a desired range of ratios.
6. Build a parametric CAD model of the mechanism.

## CHAPTER 2

# LITERATURE REVIEW

Since this work deals with a motion transmission mechanism the first part of this chapter reviews most of the existing arrangements of the continuously variable transmission (CVT). The motion transmission mechanism that is developed in the subsequent chapters is similar in nature to CVTs. Then a search for a mechanism that can change its size without changing its own shape is performed. It was found that Muray et al. [3] developed a procedure to synthesize planar mechanisms capable of approximating different shapes. Erdman et al. [4] show a diagram of a tire contractor mechanism. Both of these works do not produce a smooth change in size while maintaining their shape. Charles Hoberman [5] explains in detail a method to develop a mechanism that can change its size without changing the shape. The method is going to be used to produce a new motion transmission mechanism.

[5] Charles Hoberman patented a method to design Radial Expansion/Retraction Truss Structures [5].

### 2.1 Continuously Variable Transmission

A CVT provides an infinite number of speed ratios within the limits of the device. It is composed of an input shaft and an output shaft. The two are coupled by a belt, chain or other medium depending of the type of CVT. In the next subsections different types of CVTs will be described.

#### 2.1.1 Belt CVT and Chain CVT

Belt/chain CVT are one of the most common CVTs. Figure 2-1 shows a V-belt CVT. It consists of pulleys made out of two cones. The belt/chain goes

between the cones and has an angle to the sides. These CVTs changes its speed ratio when the cones are moved closer or apart to each other. The belt can be made out of rubber or metal depending on the application. The belt/chain can undergo both radial and tangential motions depending on the torque loading conditions and the axial forces on the pulleys. This system cannot handle high torque; new research has been done to improve this by designing metal belts that handle more loads [6] . Despite its low torque capacity, this CVT is used. It can be found on snowmobiles, go-karts and even cars (eg. Saturn Vue 2.2 L AWD (2002-2005) and Nissan Altima (from 2007, Model S))

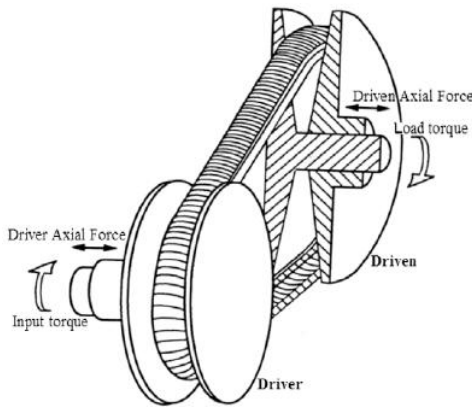


Figure 2-1: V-belt CVT [7]

Figure 2-5

### 2.1.2 Toroidal CVT

This type of CVT relies on the surface contact to transmit power. As the contact point changes in the surface, so does the speed ratio. Figure ?? shows a Toroidal CVT. It consists of two almost conical discs: one connected to the input shaft and the other connected to the output shaft. Between them are at least two rollers that transmit the power between the discs. The angle between the axis of rotation of the toroids and the axis of rotation of the discs defines the gear ratio. When they are perpendicular the input and output are the same. The drive force of this type of CVT is friction.

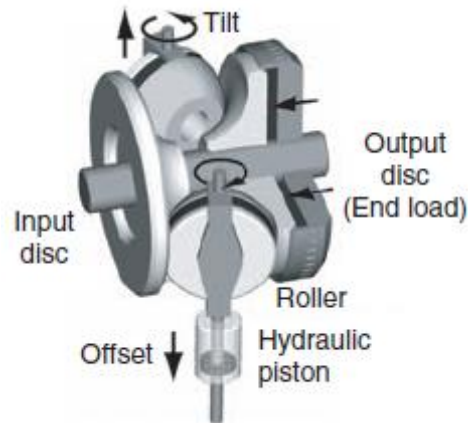


Figure 2-2: Toroidal CVT [8]

### 2.1.3 Hydrostatic CVT

Hydrostatic CVTs use hydraulic fluid to transmit power. It uses a variable displacement pump, which is the input and a hydraulic motor, which is the output. These CVTs can handle more torque than other CVTs and have the advantage that the hydraulic motor can be mounted directly to the hub of a wheel, thus having fewer losses when applied to transportation applications. One of the most common applications to these CVTs are in agricultural equipment. Figure ?? .

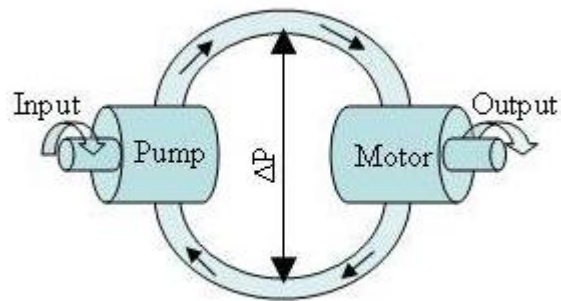


Figure 2-3: Diagram of a Hydrostatic CVT.

### 2.1.4 Ratcheting CVT

The Ratcheting CVT takes a new approach relying in static friction. These CVTs are based on elements that engage and disengage in predetermined succession between the input and output shaft. This CVT uses oscillating or indexing motion

in combination with one-way clutches or ratchets that rectify the motion. This can cause undesired vibrations through the transmission. The speed ratio is adjusted with the change in linkage geometry within the oscillating elements. Since there is no slippage, when the clutches are applied, the torque capability and efficiency of this CVT is greater than other types because of its static friction nature.

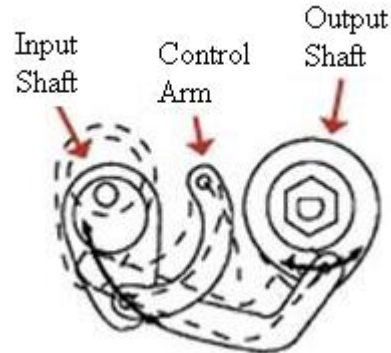


Figure 2–4: Ratcheting CVT [9]

In Figure 2–4 is an example of a ratcheting CVT. In it the output shaft has a one way clutch. The link that connects to it oscillates the clutch. In order to keep the output shaft rotating more than one array of Figure 2–4 is repeated along the shaft. That way one of the directional clutches is always engaged.

### 2.1.5 Variable Toothed Wheel Transmission

The variable toothed wheel transmission is almost a CVT. It does not change continuously its gear ratio, but it can have a large number of gear ratios. Most of these transmissions use a toothed wheel engaged to a chain. But the wheel has the ability to add or reduce the number of teeth to change the gear ratio. Since the transmission is a positive mechanical drive, it has less friction losses in the chain and other limitations related to a CVT.

Figure 2–5 shows a variable toothed wheel transmission designed by Barloworld CVT Technologies. It is composed of two conical disks, a chain with extended chain pins in contact with the sheaves, a partial drive that maintains the pitch constant and drive bars that are connected to the partial drive slots between

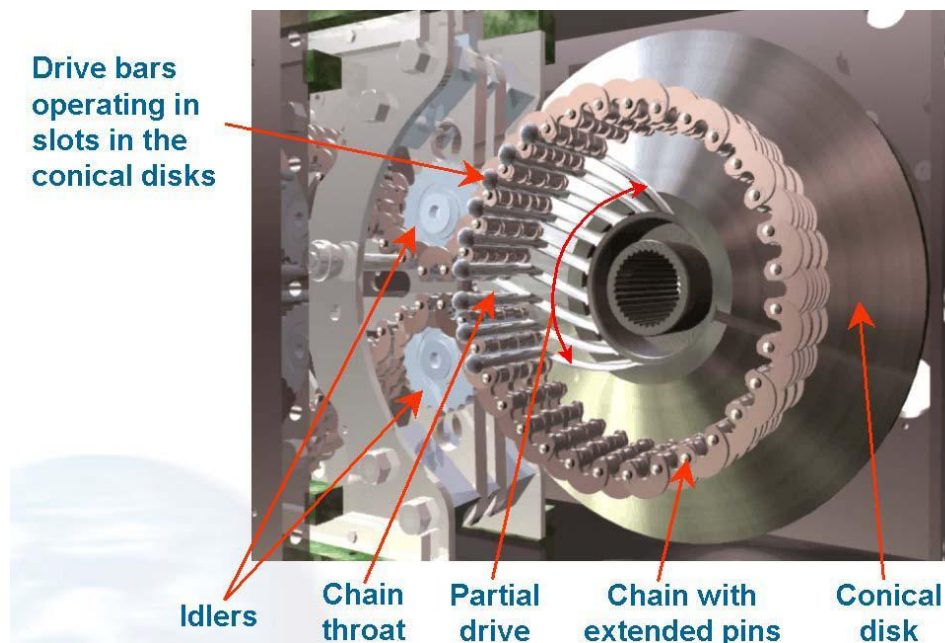


Figure 2–5: Cross-section of iCVT variator internals [10]

both conical disks. The chain forms a loop around the sheaves while entering and exiting the two idlers, this defines the chain throat. As the chain enters the chain throat and subsequently the chain loop, the chain rolls over the drive bars on the chain rollers and are positively locked in place by the chain links. The drive bars are contained in the radial slots, via their ball ends, as mentioned above and move in a radial direction together with the chain as the sheaves moves closer or further away on their rotational axial to position the chain for different ratios.

## 2.2 Hoberman Patent

Charles Hoberman patented a method to design Radial Expansion/Retraction Truss Structures [5]. In the patent he describes structures of different geometries (i.e. sphere, polygon, icosahedron) that can change gradually and smoothly their size without changing its geometry. All the connections of the structure are simple pivots. Through the patent he describes how to design truss structures of any geometric form. In the next chapter this method is applied it to a circular geometry.

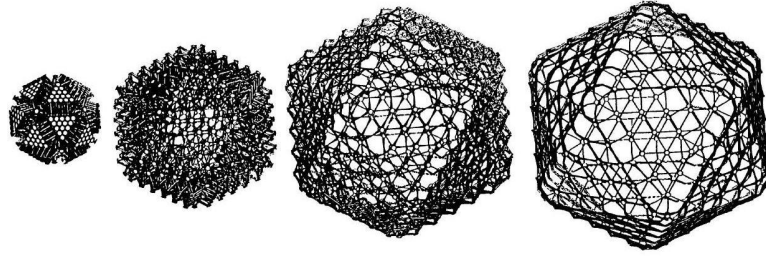


Figure 2–6: Succession of perspective views of a complete faceted icosahedral structure [5].

One example of this truss structures is shown in Figure 2–6 Where the method was applied to a faceted icosahedral. The sequence shows the shape while the size and volume of the faceted icosahedral increases.

# CHAPTER 3

## HOBBERMAN WHEEL

In this chapter we will explain the design of a circular expansion/retraction mechanism. This mechanism will be referred to as the Hoberman Wheel and/or just wheel. A perspective view of a Hoberman wheel studied in this research is shown in Figure 3-1 .

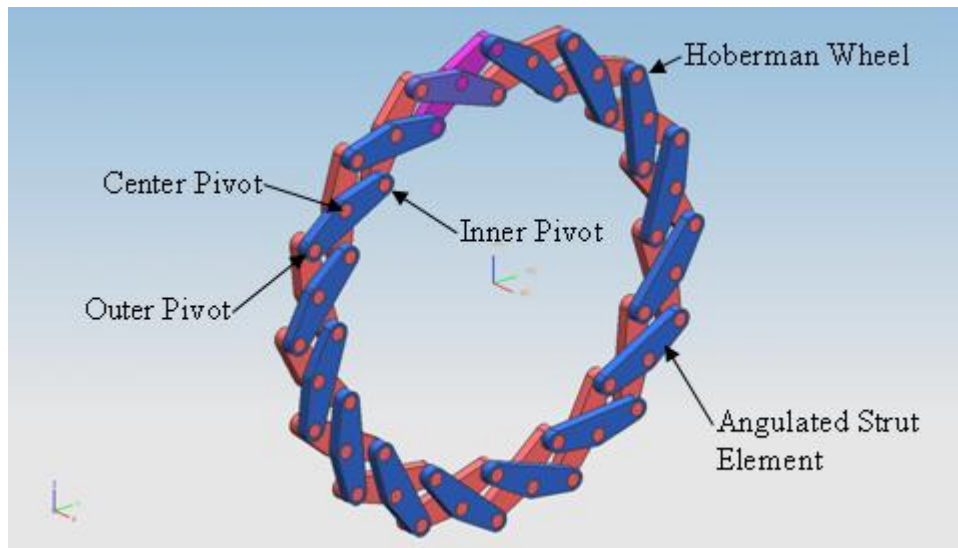


Figure 3-1: Hoberman wheel

### 3.1 Description

Figure 3-2 shows an angulated strut element. The Hoberman wheel is composed of  $2\eta$  strut elements. This strut element consists of three simple pivot points which do not lie on a straight line. The distance between the center and outer pivot points is the same. The angle  $\alpha$  created by the pivot points is the strut angle.

Two identical strut elements are coupled by their center pivot point to form a scissor pair. Figure 3-3 illustrates a scissor pair for a Hoberman wheel. The

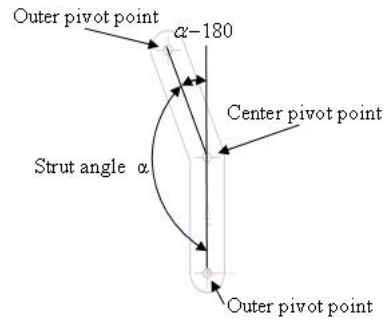


Figure 3-2: Strut element

lines drawn through a pair of outer pivot points called normal lines form the angle  $\beta$  which is the normal angle. Then  $\beta$  relates to  $\alpha$  by:

$$\alpha + \beta = 180 \quad (3.1)$$

Angle  $\beta$  does not change with the relative rotation between the strut elements. This enables the mechanism change gradually and smoothly its size without changing its geometry.

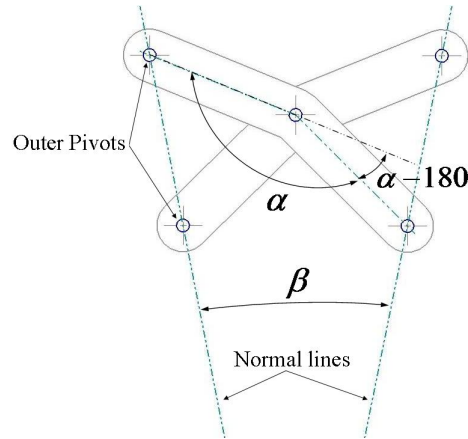


Figure 3-3: Scissor pair

The scissor pair is connected by their outer pivot points to an identical scissor pair. When  $\eta$  scissor pairs are connected together a circular form is obtained. Figure 3-4 shows an assembly of scissor pairs that together forms a circle. The number of scissor pairs, needed to complete a circle, relates to  $\alpha$  by:

$$360/(180 - \alpha) = \eta \quad (3.2)$$

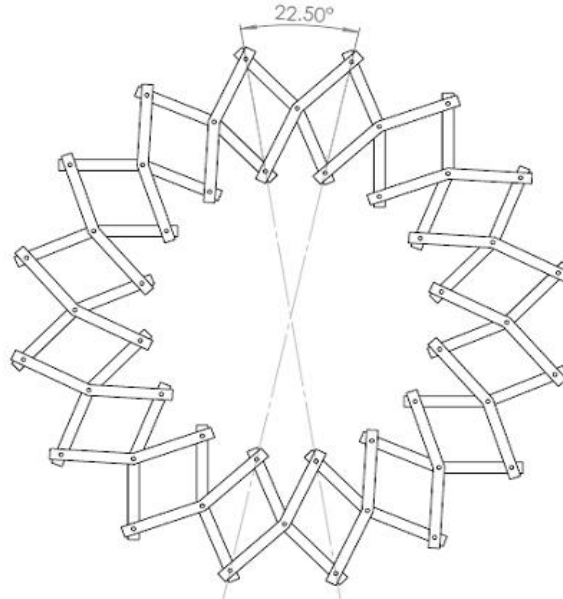


Figure 3-4: Hoberman Wheel

### 3.2 Degrees of Freedom Analysis

In order to know how many input parameters are needed to specify every position of the Hoberman wheel the degrees of freedom (DOF) are calculated. The Hoberman circle consist of  $\eta$  scissors pairs. Kutzbach-Grüblers' formula [2] is used to calculate the DOF but it does not take into account symmetry. Because of that, symmetry is exploited in the mechanism. The DOF of just one scissors pair is the DOF of the complete circle. Here we introduce the Kutzbach-Grüblers' formula for planar linkages.

$$M = -3(j - l + 1) + \sum_{n=1}^j f_i \quad (3.3)$$

Here  $M$  is the mobility,  $j$  is the number of total joints,  $l$  is the number of links or bodies, and  $\sum_{n=1}^j f_i$  is the sum of each joint's individual degree of freedom. Now counting the bodies in Figure 3-5, we have three bodies which are the two strut elements and ground. There are five joints, the center pivot point and four outer

pivot points. Each outer pivot point has two DOF and the center pivot point has only one DOF. This gives a total of 9 DOF. This information is introduced into the mobility equation (3.3) giving a mobility of zero. Equation (3.3) does not take into consideration the form (e.g. length, angles) of the bodies. This means that when equation (3.3) gives a mobility of 1, the mechanism in study will have a mobility of one for any combination of lengths. In the case of the scissor pair it has been shown [5] that for the same form for both strut elements the scissor pair is a mechanism of 1 DOF.

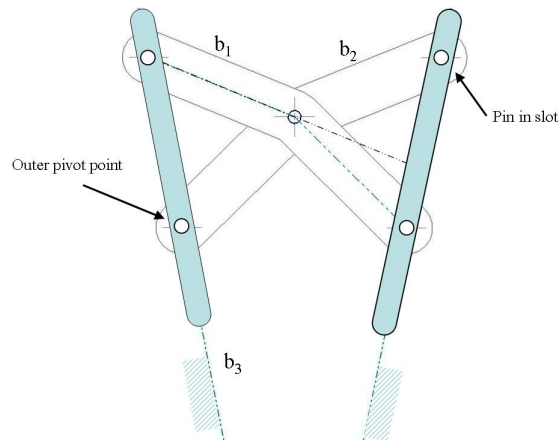


Figure 3–5: Kinematic scissor pair diagram

### 3.3 Position Vector Loop

A position vector loop is written to find the position of all the links of the wheel where the outer radius of the Hoberman wheel can be calculated. Subsequently, the maximum radius of the wheel can be found.

Figure 3–6 shows a vector loop to find the outer radius of the Hoberman wheel. As previously stated, the Hoberman circle is a mechanism of one DOF where we need one input to find the position of all parts of the mechanism.

The vector  $\vec{P}_{oa}$  is the input parameter, inner radius. This is going to be controlled by a Hoberman Circle-Shaft Mechanism. Vector  $\vec{P}_{ab}$  is the fixed distance

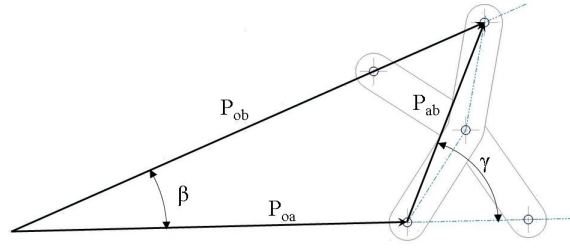


Figure 3-6: Scissor pair vector loop between the two outer pivot points. And  $\vec{P}_{ob}$  is the vector that gives the information of the length of the outer radius of the Hoberman circle. This information is summarized in equation (3.4).

$$\vec{P}_{oa} + \vec{P}_{ab} = \vec{P}_{ob} \quad (3.4)$$

In order to find the outer radius, equation (3.4) has to be solved for  $\vec{P}_{ob}$ . First we define the known vectors:

$$\vec{P}_{oa} = R_{inner} \hat{i} + 0 \hat{j} \quad (3.5)$$

$$\vec{P}_{ab} = l_{ab} \cos(\gamma) \hat{i} + l_{ab} \sin(\gamma) \hat{j} \quad (3.6)$$

$$\vec{P}_{ob} = R_{outer} \cos(\beta) \hat{i} + R_{outer} \sin(\beta) \hat{j} \quad (3.7)$$

The terms  $R_{inner}$ ,  $R_{outer}$  and  $\gamma$  are unknown. Equation (3.4) will be solved for  $R_{outer}$  in terms of  $R_{inner}$ . Thus  $\gamma$  is written in terms of  $R_{inner}$ :

$$\gamma = \arctan\left(\frac{b_x \tan(\beta) - 0}{b_x - R_{inner}}\right) \quad (3.8)$$

Where by equation (3.8) is a direct relationship between  $R_{inner}$  and  $\gamma$ . But  $b_x$  is unknown thus a relationship between it and  $R_{inner}$  is introduced using the equation of line a for line  $l_{ab}$ .

$$l_{ab} = \sqrt{(b_x - R_{inner_i})^2 + (b_x \tan(\beta) - 0)^2} \quad (3.9)$$

Due to the nature of the previous equation,  $b_x$  is obtained numerically. Then  $b_x$  is substituted into equation 3.8. With it  $\gamma$  is found and all the vectors of equation (3.4) are in terms of known values and  $R_{inner}$ . Now  $R_{outer}$  is found for different values of  $R_{inner}$ .

For plotting purposes the values in Table 3-1 are going to be used.

Table 3-1: Wheel Values Table

Name	Value
$\alpha$	157.5°
$\beta$	22.5°
$l_{ab}$	5
$\eta$	16

Figure 3-7 show a plot of  $R_{outer}$  vs  $R_{inner}$ . There we can appreciate that  $R_{outer}$  has a maximum value. Where the wheel cannot further expand.

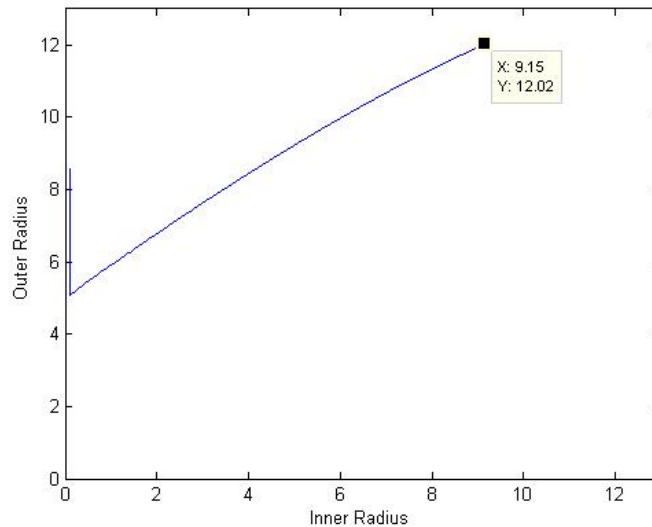


Figure 3-7: Outer radius vs inner radius of a scissor pair

Equation (3.9) is examined more closely. If  $R_{inner}$  is big enough to make the square root value bigger than  $l_{ab}$  it will result in a negative value for the scissor angle  $\lambda$ . Experimenting with the Hoberman wheel, it has been shown that  $\lambda$  increases with an increase in the inner radius and it never has a negative value.

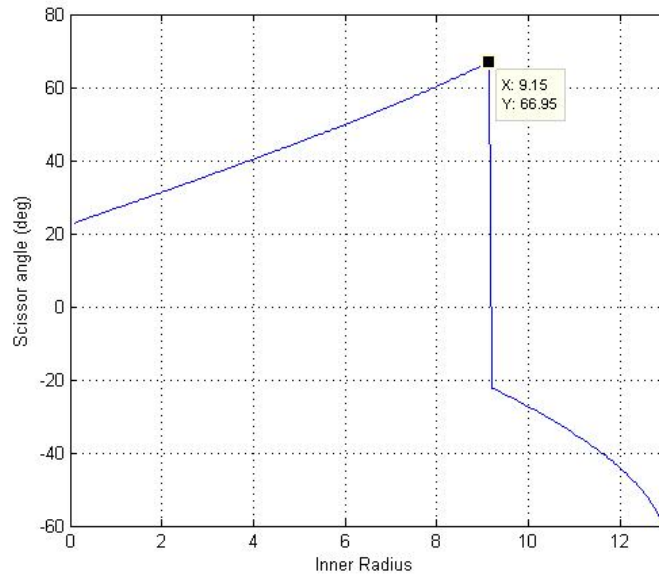


Figure 3–8: Scissor angle vs inner radius

To show more clearly the range in which the wheel works, Figure 3–8 is used. There the maximum radial distance of the wheel can be seen as it passes to a region in which the equation produces a negative  $\lambda$ . In that part the equation has a numerical solution which is not physically meaningful.

# CHAPTER 4

## VARIABLE DIAMETER WHEEL MECHANISM

An Isometric view of the variable diameter wheel (VDW) mechanism developed in this research is shown in Figure 4-1 . It is composed of a shaft, sliders, links and a Hoberman wheel.

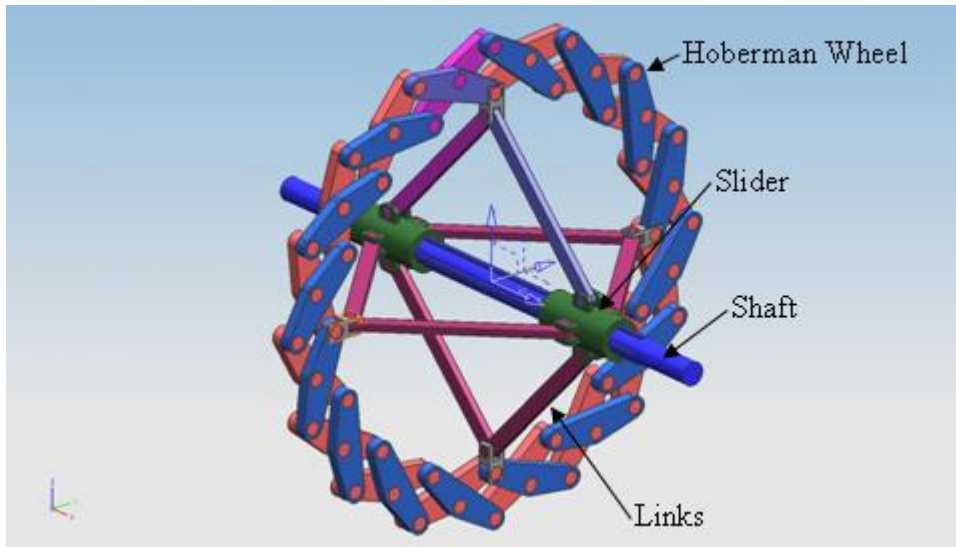


Figure 4-1: Variable diameter wheel mechanism

### 4.1 Wheel-Shaft Mechanism

The Hoberman wheel was introduced in Chapter 3. A mechanism is introduced to couple the Hoberman wheel to a rotating shaft. The resulting mechanism is one DOF. It should be noted that this coupling can be made by different mechanisms but only one is going to be presented.

A mechanism consisting of sliders and linkages is going to transmit the motion from the wheel to the shaft (see Figure 4-2 ) . Two sliders around the shaft transmit

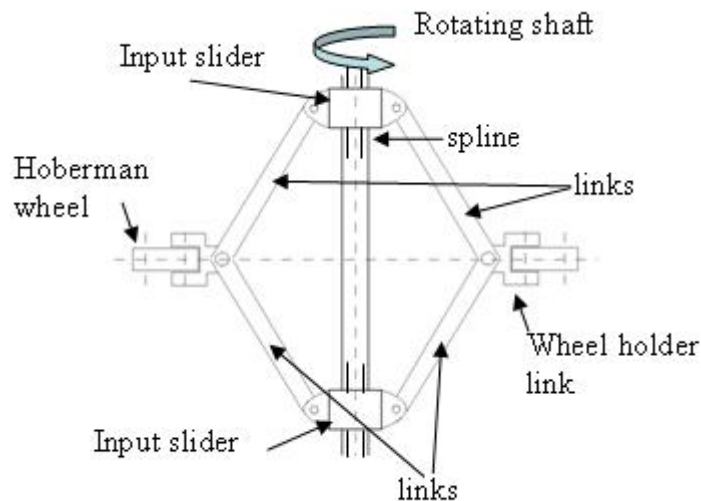


Figure 4-2: Wheel-shaft mechanism

rotation motion through a spline. A slider is located on both sides of the Hoberman wheel. These sliders are connected to links. Each link connects to a slider from one side and to the wheel holder from the other side. The wheel holder is a part that connects both link to one of the inner radius pivot points of the scissor pair. The wheel-shaft mechanism has symmetry at both sides of the wheel. This means that the links of the wheel-shaft mechanism have the same length.

#### 4.1.1 Degrees of Freedom Analysis

This slider mechanism is a one DOF. Figure 4-3 shows a simplified model for mobility analysis. Symmetry exists, therefore equation (3.3) cannot be used directly.

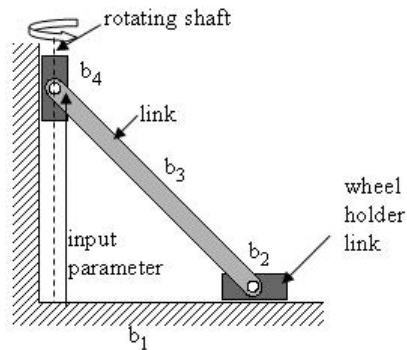


Figure 4-3: Kinematic wheel-shaft diagram

Counting the bodies in Figure 4-3, we have four bodies which are one link, two sliders, and ground. There are four joints, each joint have one DOF. This gives a total of four DOF at the joints. This information is introduced into the mobility equation (3.3) giving a mobility of one.

Now with this mechanism the radius of the wheel and “gear ratio” is controlled. Thus for now, the position of the slider (at the shaft) is the input parameter.

#### 4.1.2 Position Vector Loop

The position vector loop in Figure 4-4 has three points  $o$ ,  $c$  and  $d$ . Point  $c$  is coupled with the slider, point  $d$  is coupled with the Hoberman wheel holder and point  $o$  is at the intersection between the axis of rotation of the shaft and the plane of the wheel. The vector loop is as follows:

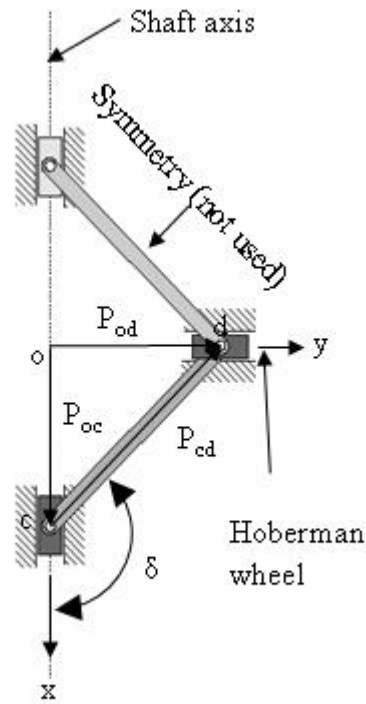


Figure 4-4: Wheel-shaft vector loop

$$\vec{P}_{oc} + \vec{P}_{cd} = \vec{P}_{od} \quad (4.1)$$

Now the definitions of each vector:

$$\overrightarrow{P_{oc}} = S_{input}\hat{i} + 0\hat{j} \quad (4.2)$$

$$\overrightarrow{P_{cd}} = l_{cd} \cos(\delta)\hat{i} + l_{cd} \sin(\delta)\hat{j} \quad (4.3)$$

$$\overrightarrow{P_{od}} = 0\hat{i} + S_{output}\hat{j} \quad (4.4)$$

Where  $S_{input}$  and  $S_{output}$  are the slider values. The vector loop equations are combined to solve for  $S_{output}$  in terms of  $S_{input}$ . The vector loop in equation (4.1) is coupled with equation (3.4) to obtain the relationship between  $\overrightarrow{P_{od}}$  and  $\overrightarrow{P_{oa}}$ . Now the input of the wheel  $R_{inner}$  is controlled by the output of the wheel-shaft mechanism  $S_{output}$  accordingly:

$$\overrightarrow{P_{oa}} = \overrightarrow{P_{od}} + l_{da} \quad (4.5)$$

In this equation  $l_{da}$  is introduced to take into account the wheel holder link (see Figure 4-4).

## 4.2 Motion Transmission Mechanism

So far the mechanism consists of a Hoberman wheel, a mechanism that couples the wheel with the shaft and a shaft. Now we will introduce a sibling mechanism as shown in Figure 4-5.

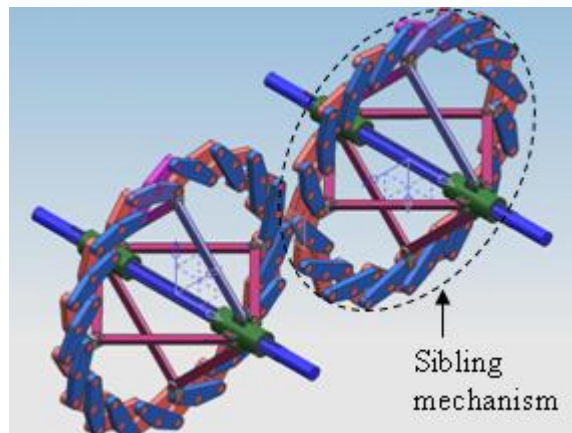


Figure 4-5: Motion Transmission Mechanism

In the assembly shown in Figure 4-5 the two shafts are parallel and the center distance between both remains constant. In order to transmit motion from one shaft to the other the outer part of both wheels has to be always in contact.

In order to explain it a nomenclature for various distances is defined in Table 4-2.

Table 4-1: Nomenclature Table

Acronym	Definition
IWSI	Input Wheel Slider Input
IWSO	Input Wheel Slider Output
IWIR	Input Wheel Inner Radius
IWOR	Input Wheel Outer Radius
OWSI	Output Wheel Slider Input
OWSO	Output Wheel Slider Output
OWIR	Output Wheel Inner Radius
OWOR	Output Wheel Outer Radius

As previously mentioned the wheel has 1 DOF which is controlled by the Wheel-Shaft mechanism. The later one has only one DOF. Since the assembly is composed of two variable diameter wheel mechanism thus it has two DOF, each DOF controls each outer radius.

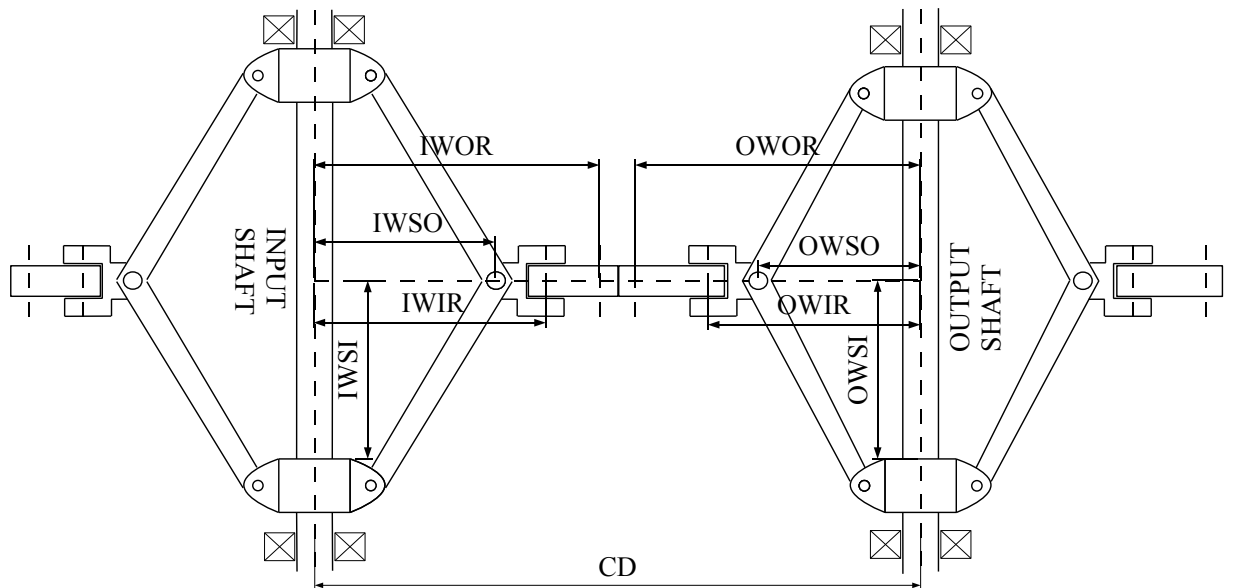


Figure 4-6: Motion transmission mechanism nomenclature diagram

### 4.3 Sliders Control Mechanism

The motion transmission mechanism has two DOF and each DOF controls the diameter of each wheel. In order to transmit motion from one axis to the other, axis, both wheels have to be in contact and thus the sum of their radius is equal to the shaft center distance. To couple the two mechanisms a slider control mechanism is proposed (Figure 4-7).

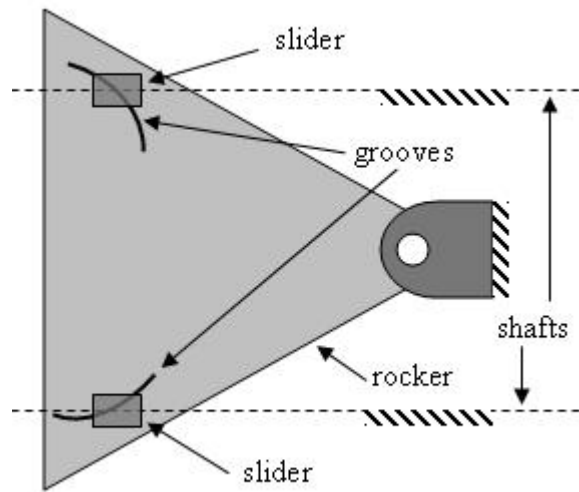


Figure 4-7: Controller mechanism diagram

#### 4.3.1 Degrees of Freedom Analysis

The control mechanism shown in Figure 4-7 has four bodies, which are a rocker, two sliders and ground. There are five joints and the sum of DOF at the joints is seven. This information is introduced into the mobility equation (3.3) giving a mobility of one. Now with the sliders control mechanism both wheels can be synchronized in order to transmit motion.

#### 4.3.2 Position Vector Loop

The position vector loop in Figure 4-8 has five points  $c_1$ ,  $c_2$ ,  $f$ , and  $g$ . Point  $c_1$  and  $c_2$  are couple to the IWSI and OWSI. These two points are the same as point  $c$  of Figure 4-4. Thus point  $c$  is couple to the slider, more specifically  $c_2$  is coupled to the IWSI and  $c_1$  is coupled to the OWSI. Point  $e$  is at the middle between the

two shafts. Points  $f$  and  $g$  are at the shafts center line aligned with each other and with point  $e$ .

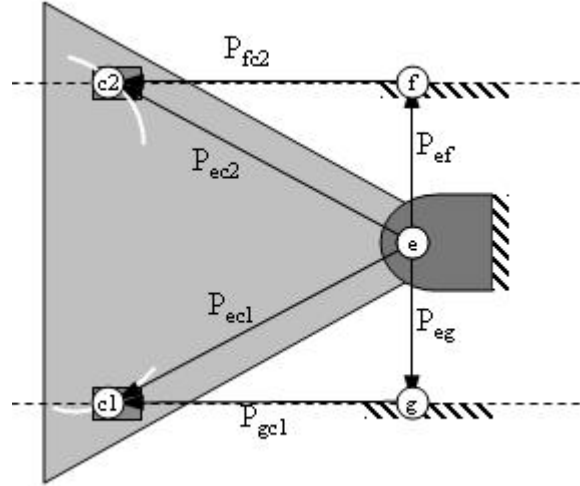


Figure 4-8: Controller mechanism vector loop

Figure 4-8 has two vector loops which are:

$$\vec{P}_{ef} + \vec{P}_{c2f} = \vec{P}_{ec2} \quad (4.6)$$

$$\vec{P}_{eg} + \vec{P}_{gc1} = \vec{P}_{ec1} \quad (4.7)$$

Now the definitions of each vector:

$$\vec{P}_{ef} = 0\hat{i} + \frac{CD}{2}\hat{j} \quad (4.8)$$

$$\vec{P}_{fc2} = (e_x - OWSI)\hat{i} + 0\hat{j} \quad (4.9)$$

$$\vec{P}_{eg} = 0\hat{i} + \frac{-CD}{2}\hat{j} \quad (4.10)$$

$$\vec{P}_{gc1} = (e_x - IWSI)\hat{i} + 0\hat{j} \quad (4.11)$$

Since all the parameters in the vector loops are known the path of the groove of the rocker can be determined to synchronize the two sliders. For this two coordinate systems are going to be used, the global coordinate system and the rocker coordinate system. The global coordinate system is located in the middle point between the shafts intersecting the plane that forms the wheels. The rocker coordinate system is located at the point where the rocker rotates.

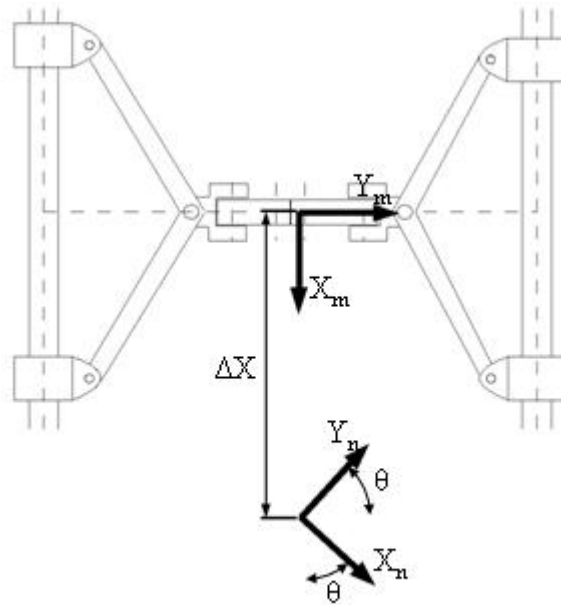


Figure 4–9: Coordinate systems diagram

With the following matrix equation one point can be represented in another coordinate system.

$$r_n = M_{nm}r_m \quad (4.12)$$

Here  $r_n$  is a four by one vector that contains the coordinates of the point in the new coordinate system. Matrix  $M_{nm}$  is the coordinate transformation matrix from coordinate system  $m$  to coordinate system  $n$ .

The matrix equation (4.13) shows a special case of the general coordinate transformation matrix [11]. In it  $\theta$  is the angle between the old and new  $x$  axis. Also it is

the angle between the old and new  $y$  axis.  $\Delta x$  is the length between the  $x_n$  axis and the  $x_m$  axis. Both angle and lengths are measured from the new coordinate system to the old coordinate system.

$$M_{nm} = \begin{pmatrix} \cos(\theta) & \sin(\theta) & 0 & \Delta x \\ -\sin(\theta) & \cos(\theta) & 0 & 0 \\ 0 & 0 & 1 & 0 \\ 0 & 0 & 0 & 1 \end{pmatrix} \quad (4.13)$$

A set of values are chosen below to plot the groove path of the rocker for the arrangement in study.

Table 4-2: Coordinate Transformation Values Table

Term	Value
$\theta_x$	$22.5^\circ \text{ to } (-22.5^\circ)$
$\theta_y$	$22.5^\circ \text{ to } (-22.5^\circ)$
$\theta_z$	$0^\circ$
$\Delta x$	-12
$\Delta y$	0
$\Delta z$	0

With a code in Matlab® the graph is obtained.

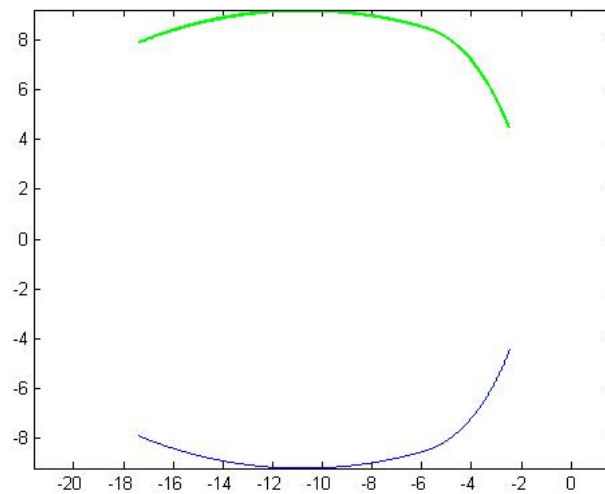


Figure 4-10: Rocker groove path.

## 4.4 Motion Transmission

### 4.4.1 Gear Ratio Range

Here the term “gear ratio” is used to define the motion transmission ratio between the two VDWs. The gear ratio for every IWSI position is calculated and shown in Figure 4–11. Figure 3–7 shows the maximum and minimum values for the outer radius of the wheel. With this information the maximum and minimum gear ratio is obtained thus finding the gear ratio range and confirming it with the range in Figure 4–11.

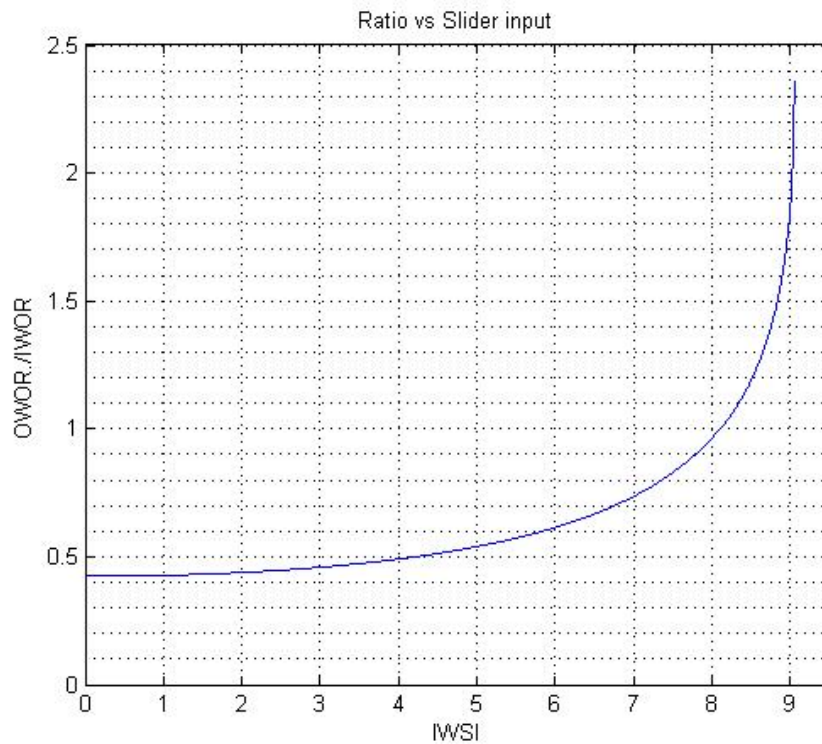


Figure 4–11: Gear ratio range for the specific arrangement.

# CHAPTER 5

## DESIGN METHODOLOGY

This chapter presents steps to design a variable diameter wheel mechanism. Since design is an iterative process, here different design iterations are presented depending on existing constraints. The code in appendix A is used for calculations.

### 5.1 Wheel Ratio Range

When there is no Center Distance ( $CD$ ) constraint the only design variables to obtain a desired ratio range are the number of scissor pairs,  $\eta$  and length of strut element,  $l_{ab}$ . The speed ratio for the variable speed ratio mechanism is defined as:

$$sr = \frac{IWOR}{OWOR} \quad (5.1)$$

Equation (5.1) is used first to calculate the minimum ratio and then the maximum ratio. The minimum ratio is the smallest outer wheel radius from Figure 3-7 divided by the maximum outer wheel radius. The maximum ratio is the inverse of the minimum ratio. Thus the minimum ratio is 0.4 and the maximum ratio is 2.5. Now the speed ratio range ( $ggr$ ) is defined as:

$$srr = \frac{gr_{max}}{gr_{min}} \quad (5.2)$$

Now with this definition  $srr$  is calculated for a range of different values of  $\eta$  and  $l_{ab}$ . The results are plotted in 5-1

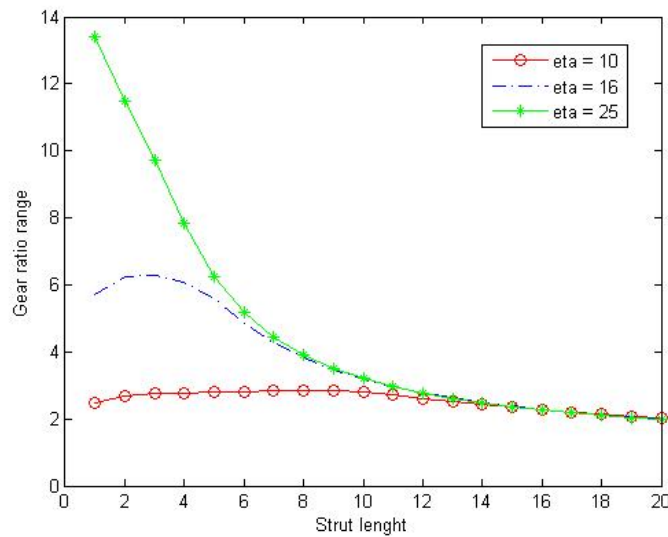


Figure 5-1: Gear ratio range vs  $\eta$  and  $l_{ab}$ .

Figure 5-1 shows that a decrease in  $l_{ab}$  and an increase in  $\eta$  increases the  $grr$ . Overall,  $l_{ab}$  has a greater effect on  $grr$  than  $\eta$ . After  $grr$  is established  $CD$  can be found.

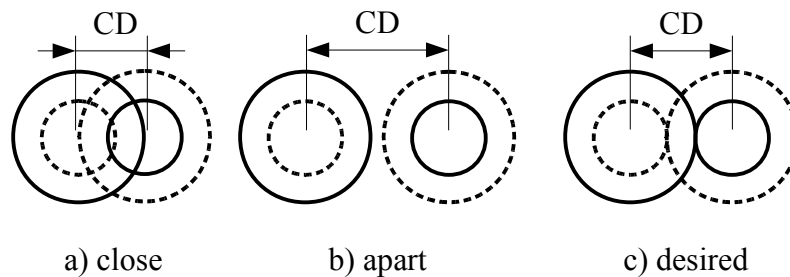


Figure 5-2: Different  $CD$

Figure 5-2 a) shows a  $CD$  in which the wheels are too close and the complete range of gear ratio is reduced. In part b) the  $CD$  is exceeds two times the maximum radius and that causes the wheels do not touch and motion can not be transmitted. Finally in part c) the  $CD$  was chosen to be the sum of the maximum radius that the wheel can expand plus the minimum radius that the wheel can contract. This ensures that the complete range of the wheel is used.

## 5.2 CD constrained

When the  $CD$  is constrained, the steps to design a variable speed ratio mechanism are different. After the  $CD$  is specified the only variable left to choose is the  $grr$ . The maximum outer radius is found with the following equation.

$$R_{max} = \frac{CD\sqrt{grr}}{1 + \sqrt{grr}} \quad (5.3)$$

Then with the maximum radius using the  $CD$  the minimum outer radius desired is found.

$$R_{min} = CD - R_{max} \quad (5.4)$$

Figure 5–3 shows that distance  $l_{ab}$  is the same as  $R_{min}$ .

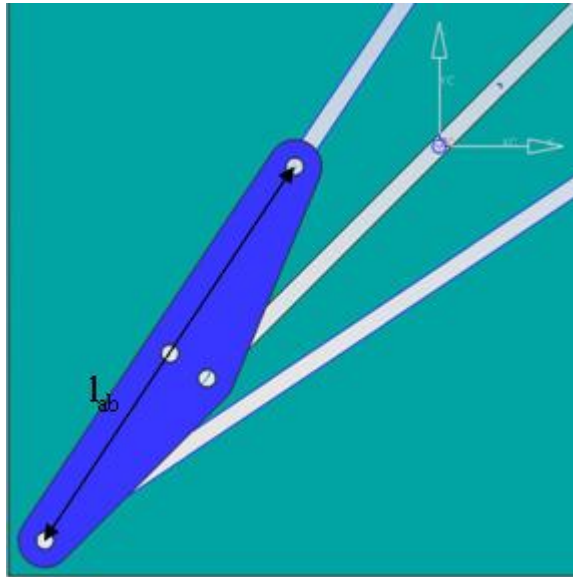


Figure 5–3: Minimum radius

Now the only term left to define the wheel is  $\eta$ . When the wheel is completely contracted, angles  $\gamma$  and  $\beta$  have the same value in equations (3.6) and (3.7). The length of  $\vec{P}_{ob}$  is:

$$l_{ab} = \sqrt{(l_{ab} \cos \beta)^2 + (l_{ab} \sin \beta)^2} \quad (5.5)$$

$\beta$  is found from equation (5.5) and by equation (3.2)  $\eta$  is calculated knowing  $\beta$ . Finally  $l_{ab}$  and  $\eta$ , which are the design parameters that define the wheels, are calculated from  $CD$  and  $grr$ .

# CHAPTER 6

## CONCLUSIONS AND FUTURE WORKS

### 6.1 Conclusions

In this thesis a VDW mechanism was developed. Further, two VDW mechanism were combined to create a variable rotation motion transmission mechanism. A kinematic analysis of the mechanism was performed. This is the first step to find the potential of the mechanism to replace a transmission in transportation equipment. Special attention was given to find the range in which it could transmit motion. The range of the ratio goes from 0.4 up to 2.5 which is similar to the gear ratio range utilized in many transmissions for transportation applications. Quasi-static load analysis of the variable ratio mechanism should be performed and afterwards structural, vibration, and fatigue analysis can be performed. The results from this analysis would yield more design constraints. It will also show the viability of using it as a transmission for transportation equipment.

### 6.2 Future Work

#### 6.2.1 Motion Transmission Mediums

In this section we will discuss how one wheel can physically transmit motion and torque to the other wheel. Here we are going to propose different mediums and explain their advantages and disadvantages.

First we are going to start with friction forces. One way that friction can be used to transmit motion and torque is to place a belt between both wheels. The belt will be compressed between the wheels, this will produce a normal force and

the surface contact between the wheel and belt can be designed in such a way that slip between both wheels does not exist.

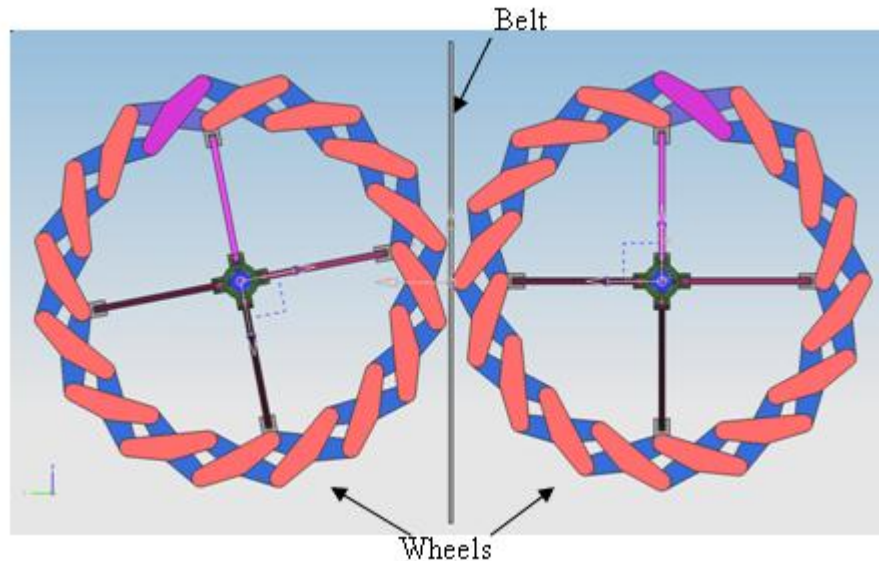


Figure 6-1: Gear ratio range for the specific arrangement.

Another arrangement that uses friction is shown in Figure 6-2. In this arrangement a flap is coupled to the outer radius pivot point of each scissor pair. This proposed flap should have a shape in a way that the mechanism resembles a circle in the best possible way at every position of the IWSI. The outer surface of the flap should have a rough finish or some sorts of material finish that result in a high friction coefficient. The drawback of this arrangement is that the gear ratio will oscillate since the form of the wheels will not be completely circular throughout the range of operation.

A very interesting arrangement would be using direct contact. This is the way gears transmit motion. The challenge is to produce a profile in the top of the wheel that meshes with the other wheel throughout the range of operation of the mechanism. If this is attained the mechanism would have an efficiency very similar to a gear pair.

The last arrangement proposed is to use Lorenz Forces. These forces can be generated with the use of magnets in the wheel. The magnetic field of the magnets

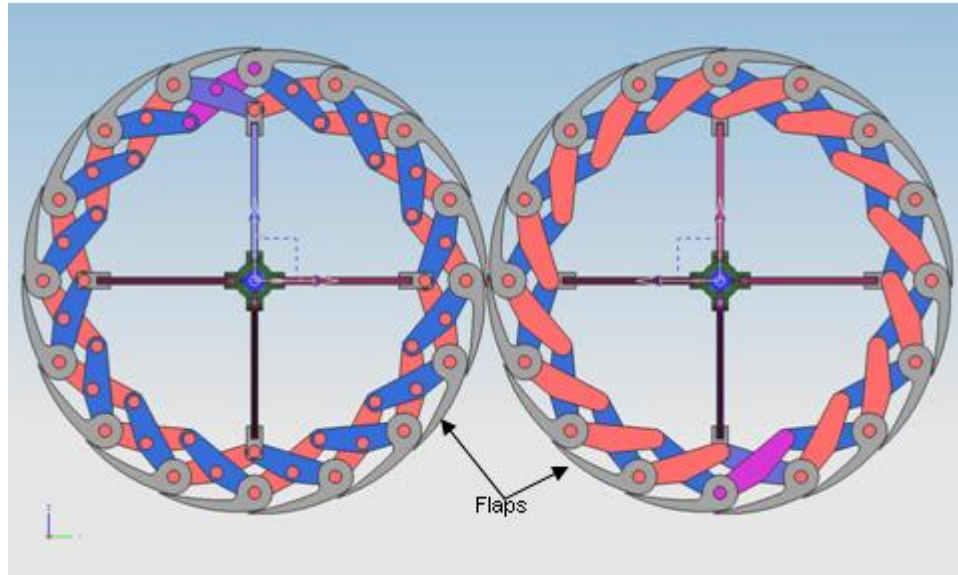


Figure 6-2: Gear ratio range for the specific arrangement.

has to be arranged in a way that the movement of one wheel is passed to the other wheel. One of the advantages of using the magnetic field is that the wheels will not actually be in contact with one another thus reducing friction losses and noise.

# APPENDICES

# APPENDIX A

## MATLABCODES

### A.1 Main Code

```
1 %%%%%%%%%%%%%%%%%%%%%%%%%%%%%%%%%%%%%%%%%%%%%%%%%%%%%%%%%%%%%%%%%%%%%%%%%%
2 % Main.Code.m %
3 % Calculates the position in the global coordinate sytem of the
4 %           complete variable diameter wheel mechanism%
5 % INPUT VARIABLES: %
6 % lab -> lenght lab of input wheel%
7 % lab2 -> lenght lab2 of input wheel%
8 % CD -> Center Distance%
9 % SInput -> slider link lenght (input)%
10 % SOutput -> slider link lenght (output)%
11 % IWSOadapter -> adapter that links IWSO with IWIR%
12 % OWSOadapter -> adapter that links OWSO with OWIR%
13 % beta -> Normal angle of Input wheel%
14 % beta2 -> Normal angle of Output wheel%
15 % presicion -> prescicion desired with secant method%
16 % maxCounter -> maximum number of iteratios for the secant method%
17 % IWSIstart -> starting value of IWSI%
18 % IWSIend -> end value of IWSI%
19 % IWSIinterval -> interval of IWSI%
20 %
21 % LOCAL VARIABLES: %
22 % ii, jj, qq, rr -> For-loop indices %
```

```

23 %
24 % OUTPUT VARIABLES: %
25 % IWSI -> Input wheel slider inputs %
26 % IWSO -> Input wheel Slider Output %
27 % IWIR -> Input Wheel Inner Radius %
28 % bi -> x coordinate of point b %
29 % bj -> bj is the y coordinate of point b %
30 % lambda -> angle at which the scissor element is lean %
31 % IWOR -> Input wheel outer radius %
32 % OWOR -> Output wheel outer radius %
33 % OWIR -> Output Wheel Inner radius %
34 % OWSO -> Output Wheel Slider Output %
35 % OWSI -> Output wheel Slider Input %
36 %
37 % THIS FUNCTION IS CALLED FROM: %
38 %     none%
39 % THIS FUNCTION CALLS: %
40 % SecantMethodFuncSpecial.m %
41 %
42 %%%%%%%%%%%%%%%%%%%%%%%%%%%%%%%%%%%%%%%%%%%%%%%%%%%%%%%%%%%%%%%%%%%%%%%%%%
43 clear all
44 clc
45 %input (lenght parameters)
46 lab = 5;
47 lab2 = 5;
48 CD = 17.1149;
49 %CD calculated(max outer radius + min outer radius)%max(IWOR)+min(IWOR)
50 %CD value guess in first iteration
51 SLinput = 9.05;
52 SLoutput = 9.05;
53 IWSOadapter = 0.1;
54 OWSOadapter = 0.1;
55 %input (angle parameters)

```

```

56 beta = 22.5*(pi/180);
57 beta2 = 22.5*(pi/180);
58 %input (miscelaneous)
59 bj = 0;
60 ii=0;           %counter star value
61 presicion = 0.00001;
62 maxCounter = 200;
63 IWSIstart = 0;
64 IWSIend = SLinput;
65 IWSIinterval = 0.005;
66 %Functions used in secant method
67 fun = @(bi,r) ((bi-r)^2+(bi*tan(beta))^2)-lab^2;
68 %function Input Wheel 1 (outer radius)
69 fun3 = @(bi2,r) ((bi2-r).^2+(bi2.*tan(beta2)).^2)-lab2.^2;
70 %function Output Wheel (outer radius)
71 fun2 = @(bi2,r) (((r.*cos(beta2))-bi2).^2+(r.*sin(beta2)).^2)-lab2.^2;
72 %function Output Wheel (inner radius)
73 for IWSI = IWSIstart:IWSIinterval:IWSIend
74     ii=ii+1;     %counter increment
75     IWSO(ii) = (SLinput^2-IWSI^2)^(1/2);
76 end
77 IWIR = IWSO + IWSOadapter;
78 for jj = 1:ii
79     %Input wheel inner radius
80     x0= 5;       %starting values for secant method
81     x1= 10;      %starting values for secant method
82     bi(jj) = SecantMethodFuncSpecial(fun,IWIR(jj),x0,x1,presicion,maxCounter);
83     bj(jj) = bi(jj)*tan(beta);
84     lambda(jj) = atan((bj(jj)-bj)/(bi(jj)-IWIR(jj)));
85     IWOR(jj) = (bi(jj)^2+bj(jj)^2)^(1/2);
86     %start of output wheel
87     OWOR(jj) = CD - IWOR(jj);
88     OWIR(jj) = SecantMethodFuncSpecial(fun2,OWOR(jj),-2,-1,presicion,maxCounter);

```

```

89     %finish of output wheel
90 OWSO(jj) = OWIR(jj) - IWSOadapter;
91 OWSI(jj) = (SLoutput^2-(OWSO(jj))^2)^(1/2);
92 end
93 %postprocesor
94 qq = 1;
95 rr = 1;
96 IWSI = IWSIstart:IWSIinterval:IWSIend;
97 for jj= ii:-1:2
98     if lambda(jj)*(180/pi)<lambda(jj-1)*(180/pi)
99         rangeend(qq) = jj;
100         qq = qq + 1;
101     end
102     if IWOR(jj)+lac2(jj)== 20
103         rr = rr +1;
104         rangestart(rr)=jj;
105     end
106 end

```

## A.2 Secant Method Function

```

1 function [x2]=SecantMethodFuncSpecial(fun,r,x0,x1,presicion,maxCounter)
2 %%%%%%%%%%%%%%%%%%%%%%%%%%%%%%%%%%%%%%%%%%%%%%%%%%%%%%%%%%%%%%%%%%%%%%%%%
3 % SecantMethodFunc.m %
4 % Calculates the zeros of the function%
5 % INPUT VARIABLES: %
6 % fun -> function %
7 % r -> fun second input value %
8 % x0, x1 -> start value of secant method %
9 % presicion -> presicion desired %
10 % maxCounter -> maximum number of iterations to exit loop %
11 % LOCAL VARIABLES: %

```

```

12 % counter -> For-loop indices %
13 % OUTPUT VARIABLES: %
14 % x2 -> zero of function fun %
15 % THIS FUNCTION IS CALLED FROM: %
16 % thessis5.m %
17 % THIS FUNCTION CALLS: %
18 % Doesn t call any FUNCTION %
19 %%%%%%%%%%%%%%%%%%%%%%%%%%%%%%%%%%%%%%%%%%%%%%%%%%%%%%%%%%%%%%%%%%%%%%%%%%
20 counter = 1;
21 while (abs(fun(x0,r))>presicion && counter<maxCounter)
22     x2 = x1 - (x1-x0)/(fun(x1,r)-fun(x0,r))*fun(x1,r);
23     x0 = x1;
24     x1 = x2;
25     counter = counter + 1;
26 end
27 x2;

```

### A.3 Gear ratio range

```

1 %%%%%%%%%%%%%%%%%%%%%%%%%%%%%%%%%%%%%%%%%%%%%%%%%%%%%%%%%%%%%%%%%%%%%%%%%%
2 % gearratorange.m %
3 % Calculates the grr for every IWSI for a range of lab and
4 % eta combinations%
5 % INPUT VARIABLES: %
6 % etasize -> size and range of eta %
7 % labsize -> size and range of lab %
8 % OUTPUT VARIABLES: %
9 % Range -> matrix with grr values for various eta and lab %
10 % THIS FUNCTION IS CALLED FROM: %
11 % N/A %
12 % THIS FUNCTION CALLS: %
13 % MaxMinRad.m %

```

```

14 %%%%%%%%%%%%%%%%%%%%%%%%%%%%%%%%%%%%%%%%%%%%%%%%%%%%%%%%%%%%%%%%%%%%%%%%%
15 clear all
16 clc
17
18 [xxx,etasize]=size(10:60);
19 [xxx,labsize]=size(1:20);
20 Range=zeros(etasize,lbcsize);
21 Min=zeros(etasize,labsize);
22 Max=zeros(etasize,labsize);
23
24 for eta = 10:60
25
26     for lab = 1:20
27
28         [Min(eta,lab),Max(eta,lab)]=MaxMinRad(eta,lab);
29
30         Range(eta,lab) = ((Max(eta,lab)/Min(eta,lab))/(Min(eta,lab)/Max(eta,lab)));
31     end
32 end
33 surf(Range)

```

#### A.4 Maximum and Minimum radius function

```

1 %%%%%%%%%%%%%%%%%%%%%%%%%%%%%%%%%%%%%%%%%%%%%%%%%%%%%%%%%%%%%%%%%%%%%%%%%
2 % %
3 % MaxMinRad.m %
4 % %
5 % Calculates the Maximun and Minimum radius for a VDW %
6 % INPUT VARIABLES: %
7 % eta -> number of scissor pairs%
8 % lbc -> lenght of strut element%
9 %

```

```

10 % LOCAL VARIABLES: %
11 % ii -> for-loop indices %
12 % rin -> starting value of r
13 % rend -> last value of r
14 % rinterval -> %interval of r
15 % presicion -> prescicion desired with secant method%
16 % maxCounter -> maximum number of iteratios for the secant method%
17 % fun -> VDW outer radius function for secant method%
18 % bit -> if condition%
19 % OUTPUT VARIABLES: %
20 % bi -> x coordinate of point b %
21 % bj -> bj is the y coordinate of point b %
22 % lambda -> angle at which the scissor element is lean %
23 % Min -> Minimum radius %
24 % Max -> Maximum radius %
25 % THIS FUNCTION IS CALLED FROM: %
26 % gearratorange.m      %
27 % THIS FUNCTION CALLS: %
28 % SecantMethodFuncSpecial.m %
29 % %
30 %%%%%%%%%%%%%%%%%%%%%%%%%%%%%%%%%%%%%%%%%%%%%%%%%%%%%%%%%%%%%%%%%%%%%%%%%%
31 function [Min,Max]=MaxMinRad(eta,lbc);
32 alpha = (360/eta)*(pi/180);
33 r= 0.2;      %debug purpose
34 rin=0.1;
35 rend=20;
36 rinterval = 0.05
37 fun = @(ci,r)((ci-r)^2+(ci*tan(alpha))^2)-lbc^2;
38 presicion = 0.0001;
39 maxCounter = 200;
40 ii=1;
41 bit = 0;
42 for r = rin:rinterval:rend

```

```

43     x0= 5;
44     x1= 10;
45     bi(ii) = SecantMethodFuncSpecial(fun,r,x0,x1,presicion,maxCounter);
46     bj(ii) = bi(ii)*tan(alpha);
47     lambda(ii) = atan((bj(ii)-0)/(bi(ii)-r));
48     IWOR(ii) = (bi(ii)^2+bj(ii)^2)^(1/2);
49     if ii>2
50         if lambda(ii)< lambda(ii-1) && bit ==0
51             Max = IWOR(ii-1);
52             bit = 1;
53         end
54     end
55     ii=ii+1;
56 end
57 Min = lac(1);

```

## A.5 Maximum and Minimum radius function

```

1  %%%%%%%%%%%%%%%%%%%%%%%%%%%%%%%%%%%%%%%%%%%%%%%%%%%%%%%%%%%%%%%%%%%%%%%%%%%
2  % %
3  % CDconstrained.m%
4  % Calculates lab and beta with CD and grr as inputs %
5  % INPUT VARIABLES: %
6  % CD -> Center Distance%
7  % grr -> Gear Ratio Range%
8  % eta -> number of scissor pairs%
9  % lbc -> lenght of strut element%
10 % LOCAL VARIABLES: %
11 % ii -> for-loop indices %
12 % rin -> starting value of r
13 % rend -> last value of r
14 % rinterval -> %interval of r

```

```

15 % presicion -> prescicion desired with secant method%
16 % maxCounter -> maximum number of iteratios for the secant method%
17 % fun -> VDW outer radius function for secant method%
18 % bit -> if condition%
19 % OUTPUT VARIABLES: %
20 % eta -> number of scissor pairs%
21 % lbc -> lenght of strut element%
22 % bi -> x coordinate of point b %
23 % bj -> bj is the y coordinate of point b %
24 % lambda -> angle at which the scissor element is lean %
25 % Min -> Minimum radius %
26 % Max -> Maximum radius %
27 % THIS FUNCTION IS CALLED FROM: %
28 % gearratorange.m      %
29 % THIS FUNCTION CALLS: %
30 % SecantMethodFuncSpecial.m %
31 %%%%%%%%%%%%%%%%%%%%%%%%%%%%%%%%%%%%%%%%%%%%%%%%%%%%%%%%%%%%%%%%%%%%%%%%%%
32 clear all
33 clc
34 CD = 14;
35 grr = 6;
36 rmax = (grr^(1/2)*CD)/(1+(grr)^(1/2));
37 rmin = CD-rmax;
38 lab = rmin;
39 r= 0.2;      %debug purpose
40 rin=0.1;    %starting value of r
41 rfin=20;    %last value of r
42 rinterval = 0.05; %interval of r
43 fun = @(beta) ((lab.*cos(beta)).^2+(lab.*cos(beta)).^2)-lab.^2;
44 presicion = 0.0001;
45 maxCounter = 200;
46 x0= 0.1;
47 x1= 0.5;

```

```
48 beta = SecantMethodFuncSpecialCD(fun,x0,x1,presicion,maxCounter);  
49 beta = beta*(180/pi);  
50 eta = 360/beta;  
51 lab
```

# APPENDIX B NX 5 MODELS

## B.1 Screen shots of NX 5 Model changing ratios

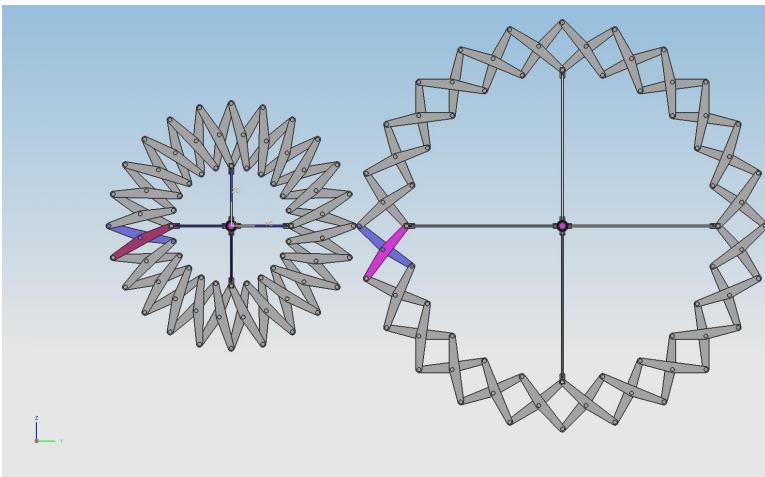


Figure B-1:

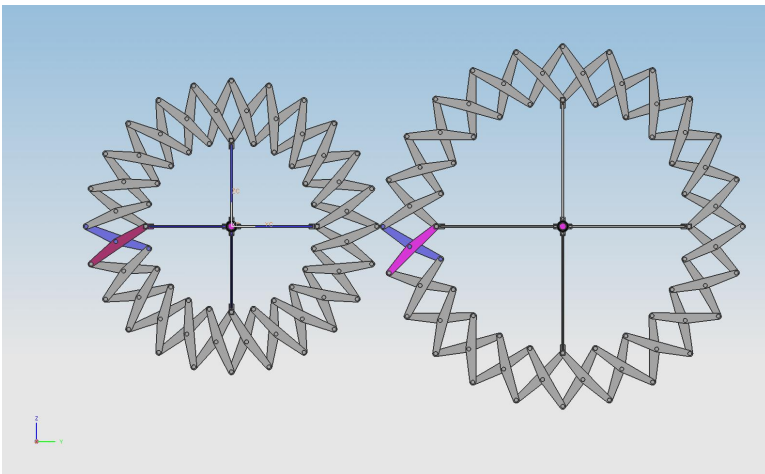


Figure B-2:

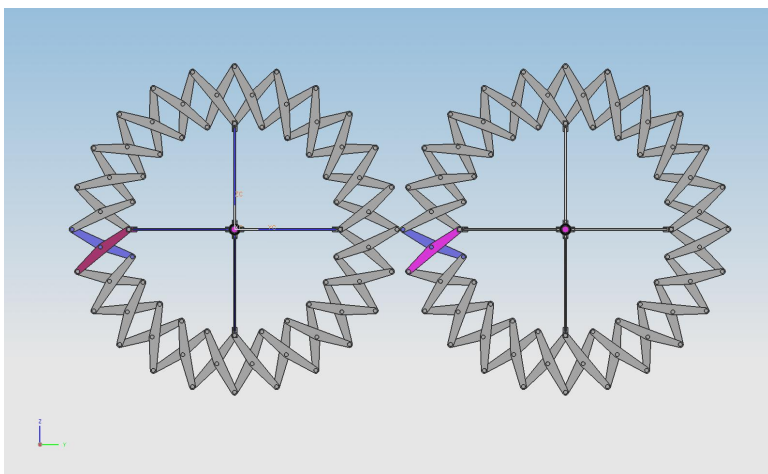


Figure B-3:

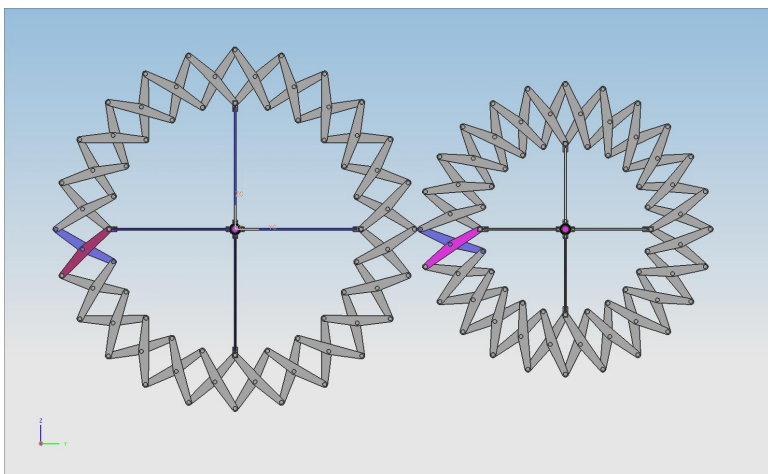


Figure B-4:

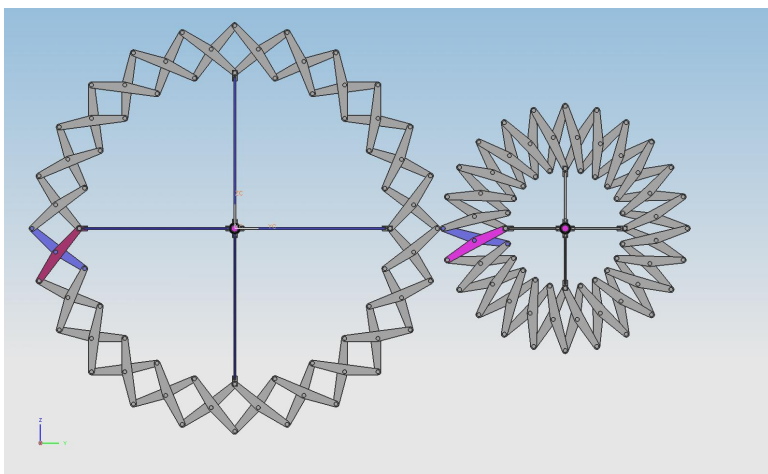


Figure B-5:

## REFERENCE LIST

- [1] Andreas Shafer David L. Greene. Reducing greenhouse gas emissions from u.s. transportation. Technical report, Pew Center on Global Climate Change, 2003.
- [2] Robert L. Norton. *Design of Machinery*. Mc Graw Hill, second edition, 2001.
- [3] Andrew P. Murray, James P. Schmiedeler, and Brian M. Korte. Kinematic synthesis of planar, shape-changing rigid-body mechanisms. *Journal of Mechanical Design*, 130(3):032302, 2008.
- [4] Sridhar Kota Arthur G. Erdman, George N. Sandor. *Mechanism Design: Analysis and Synthesis*. Prentice Hall, 4 edition, May 2001.
- [5] Charles Hoberman. Radial expansion\retraction truss structures, Jun 1991.
- [6] C.R. Burrows J.D. Micklem, D.K. Longmore. Modelling of the steel pushing v-belt continuously variable transmission. *Proceedings of the Institution of Mechanical Engineers, Part C: Journal of Mechanical Engineering Science*, 208:13–27, 1994.
- [7] Imtiaz Haque Nilabh Srivastava. A review on belt and chain continuously variable transmissions (cvt): Dynamics and control. *Mechanism and Machine Theory*, 44(1):19–41, Jan 2009.
- [8] Y. Rothernbuehler K. Matsumoto R. Fuchs, Y. Hasuda. Control concepts of continuously variable transmissions (cvt). Technical report, JTEKT Engineering, 2006.
- [9] Zero-max home page, Mar 2009. [online] <http://www.zero-max.com/products/drives/drivesmain.asp>.
- [10] Dr. Jan Naude. Development of a positive drive icvt (incremental continuously variable transmission). Technical report, Barloworld CVT Technologies.

- [11] Faydor L. Litvin. *Gear Geometry and Applied Theory*. Prentice Hall, first edition, 1994.